arXiv:1404.2721v1 [physics.optics] 10 Apr 2014

Optimal preselection and postselection in weak measurements for observing photonic spin Hall effect

Xinxing Zhou,[1] Xing Li,[1] Hailu Luo,[1, a)] and Shuangchun Wen[1, b)]
Key Laboratory for Micro-/Nano-Optoelectronic Devices of Ministry of Education, College of Physics and Microelectronic Science, Hunan University, Changsha 410082, People's Republic of China

(Dated: 11 April 2014)

Photonic spin Hall effect (SHE) holds great potential applications in precision metrology. How to obtain a high measurement precision is an important issue to detect the photonic SHE. In this letter, we propose using optimal preselection and postselection in weak measurements to enhance the measurement precision. We find that the maximum weak value and pointer shift can be obtained with an optimal overlap of preselection and postselection states. These findings offer the possibility for improving the precision of weak measurements and thereby have possible applications for accurately characterizing the parameters of nanostructures.

After first proposed by Aharonov, Albert, and Vaidman (AAV)[1] in 1988, the weak measurements based on preselection and postselection states has been a promising method for helping us in investigating fundamental questions of quantum mechanics[2–4]. The idea of weak measurements can be described as follows: if we initially select the quantum system with a well-defined preselection state, the corresponding large expectation values can be obtained with a suitable postselection state, which makes the eigenvalues to be clearly distinguished. Recently, the weak measurements has been useful for precision measurement such as detecting very small transverse beam deflections[5], observing photonic spin Hall effect (SHE)[6–9], determining the average trajectories of single photons[10], direct measurement of the quantum wavefunction[11], and measuring ultrasmall time delays of light[12].

The photonic SHE is attributed to spin-orbit coupling and manifests itself as spin-dependent splitting[13–20]. The photonic SHE is sensitive to the variations of physical system's states and holds great potential applications in precision metrology, such as probing spatial distributions of electron spin states[21], measuring the thickness of nanometal film[22], identifying graphene layers[23], and detecting the axion coupling in topological insulators[24]. The spin-dependent splitting of photonic SHE in these systems is just a few tens of nanometers and the weak measurement method is usually used to probe this phenomenon. However, in the process of weak measurements for probing the photonic SHE, how to get the large amplified factor is an important issue for enhancing the measurement precision.

In this letter, we propose using optimal preselection and postselection in weak measurements to detect the photonic spin Hall effect (SHE) for obtaining the maximum outcome. We consider the regime of preselection and postselection being almost orthogonal. It is found that, for a fixed incident angle, the maximum amplified factor and pointer shift (amplified displacement of photonic SHE) can be obtained with a corresponding optimal overlap of preselection and postselection states. Therefore, we can significantly improve the precision of weak measurements for probing the photonic SHE. We also find that, under the orthogonal condition of preselection and postselection states, the amplified factor and amplified shift can not be arbitrarily large and, on the contrary, they turn out to be zero. The experimental results agree well with our theoretical discussions.

In general, the amplified factor is corresponding to the so-called weak value which establishes the relationship between the observable and the shifts in measurement pointer's mean position and mean momentum[25]

$$A_w = \frac{\langle\psi_2|\hat{\mathbf{A}}|\psi_1\rangle}{\langle\psi_2|\psi_1\rangle}. \tag{1}$$

ψ_1 and ψ_2 denote the preselection and postselection states. When $\langle\psi_2|\psi_1\rangle\to 0$, the weak value might become arbitrarily large. However, arbitrarily large results in photonic SHE can not be obtained and we need to choose an appropriate preselection and postselection states for obtaining the maximum weak value. Some theoretical works have been done to discuss this phenomena[26–28], however, there lacks specific experiment and the photonic SHE is not considered.

Figure 1 schematically draws the photonic SHE of light beam reflection from a planar interface and the corresponding weak measurement process. The incident polarization states are chosen as $|H\rangle$ and $|V\rangle$. This polarization selection can be seen as the preselection process in weak measurements, which is discussed in the following. In the spin basis, the horizontal and vertical polarization states can be expressed as $|H\rangle = (|+\rangle + |-\rangle)/\sqrt{2}$ and $|V\rangle = i(|-\rangle - |+\rangle)/\sqrt{2}$. In the spin basis, the states of reflected beam can be obtained:

$$|H\rangle \to \frac{r_p}{\sqrt{2}}\left[\exp(+ik_{ry}\delta_r^H)|+\rangle + \exp(-ik_{ry}\delta_r^H)|-\rangle\right], \tag{2}$$

a) Electronic mail: hailuluo@hnu.edu.cn
b) Electronic mail: scwen@hnu.edu.cn

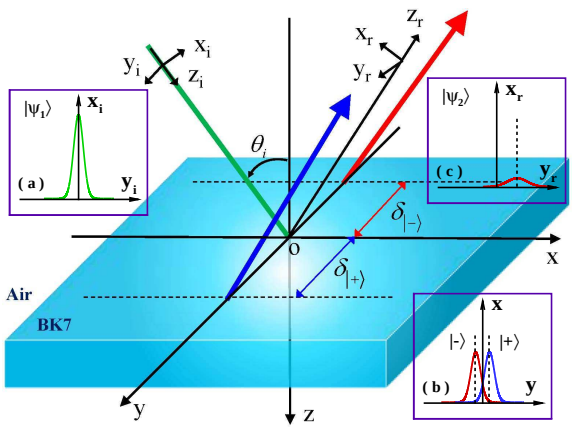

FIG. 1. (Color online) Schematic of photonic SHE on a BK7 prism interface and the corresponding weak measurement process. A linearly polarized beam reflects on the prism and then splits into left- and right-handed circularly polarized light, respectively. $\delta_{|+\rangle}$ and $\delta_{|-\rangle}$ denote the transverse shifts of left- and right-handed circularly polarized components. Here, θ_i is the incident angle and the insets show the three steps of weak measurements: (a) preselection, (b) weak coupling between observable and meter, and (c) postselection.

$$|V\rangle \rightarrow \frac{ir_s}{\sqrt{2}}\left[-\exp(+ik_{ry}\delta_r^V)|+\rangle + \exp(-ik_{ry}\delta_r^V)|-\rangle\right]. \tag{3}$$

In the above equations, $\delta_r^H = (1 + r_s/r_p)\cot\theta_i/k_0$, $\delta_r^V = (1 - r_p/r_s)\cot\theta_i/k_0$.

The photonic SHE manifests for the spin-dependent splitting of left- and right-handed circularly polarized components. Here we only consider the spin separation in the y direction (transverse shift). In the following, we calculate the shifts of these two spin components. The wavefunction of reflected photons is composed of the packet spatial extent $\phi(k_{ry})$ and the polarization description $|H, V\rangle$:

$$|\Phi^{H,V}\rangle = \int dk_{ry}\phi(k_{ry})|k_{ry}\rangle|H, V\rangle. \tag{4}$$

After photons reflection from the interface, the initial state $|\Phi_{inital}^{H,V}\rangle$ evolve into the final state $|\Phi_{final}^{H,V}\rangle$. As a result of spin-orbit coupling, the displacements of the two spin components compared to the geometrical-optics prediction are given by

$$\delta_{|\pm\rangle}^{H,V} = \frac{\langle\Phi^{H,V}|i\partial_{\mathbf{k}_\perp}|\Phi^{H,V}\rangle}{\langle\Phi^{H,V}|\Phi^{H,V}\rangle}. \tag{5}$$

Here, we suppose the $\phi(k_{ry})$ is a Gaussian wave function.

In the process of quantum weak measurements, the property observable of a system is first coupled to the meter (measuring device), and then the information about the state of the observable is read out from the meter. In the case at hand, the detection of photonic SHE induced transverse shifts is actually equivalent to a quantum measurement of the spin degree of freedom along the central propagation direction corresponding to the observable $\hat{\sigma}_3$, with the transverse spatial distribution serving as the meter[6]. This can be done through three steps. Firstly, the system is prepared with a fixed preselection state ψ_1. In the present work, the incident polarization states are chosen as $|H\rangle$ and $|V\rangle$. And then, with the weak interaction, the observable (left- or right-handed circularly polarized component) is coupled to the transverse spatial distribution of the Gaussian wave function with the Hamiltonian interaction. Finally, an enhanced shift in the meter distribution can be obtained with the suitable postselection state $|\psi_2\rangle = |V \pm \Delta\rangle$ or $|H \pm \Delta\rangle$ of the observable. Here, the $\Delta \ll 1$ is a small angle. The last step can also be seen as the strong measurement. When the Δ is close to zero, the preselection and postselection states are almost orthogonal.

Our experimental setup is similar to that in Ref.[9] and the detail equipment description and experimental analysis can be found. Our sample is an usual BK7 prism. The amplified displacements can be obtained through the preselection and postselection process, and so we can get the relationship between the final position of the meter and the observable $\hat{\mathbf{A}}$ by the weak value A_w. A Gauss beam generated by He-Ne laser is firstly focused by the lens (L1) and experiences preselection in the state $|\psi_1\rangle$=$|H\rangle$ or $|V\rangle$ with the polarizer P1. When the light beam reflects from the prism interface, the photonic SHE happens allowing for the left- and right-handed circularly polarized components splitting in the y direction. This process is the weak interaction allowing for the coupling between the observable and the meter. And then the beam passes through the second polarizer P2 preparing for the postselection state $|\psi_2\rangle = |V \pm \Delta\rangle$ or $|H \pm \Delta\rangle$. We can obtain the reflected field at the plane of z_r. At the surface of the second polarizer, the two circular polarization components experience destructive interference making the enhanced shift $\delta_w^{H,V}$ in the meter much larger than the initial one $\delta_{|\pm\rangle}$. Calculating the reflected field distribution yields the amplified shifts of photonic SHE. After passing through the second lens (L2), a CCD is used to capture the optical signal and measure the amplified shifts. The process discussed above is called the weak value amplification and Δ is the postselection angle.

In terms of weak value amplification, the preselection and postselection states $|\psi_1\rangle$ and $|\psi_2\rangle$ determine the weak value A_w of the photon helicity. We should note that the imaginary weak value also corresponds to a shift of the meter in momentum space, which leads to the possibility of even larger enhancements following the beam free evolution[6]. This process can be seen as propagation amplification that produces the amplified factor F. The propagation amplified factor depends on the initial state of the beam and the degree of its free evolution before the observer. Therefore, under this condition, we can also get the final shift of the meter as the modified weak value $A_w^{mod} = |A_w|F$. From the calculation, we can obtain the

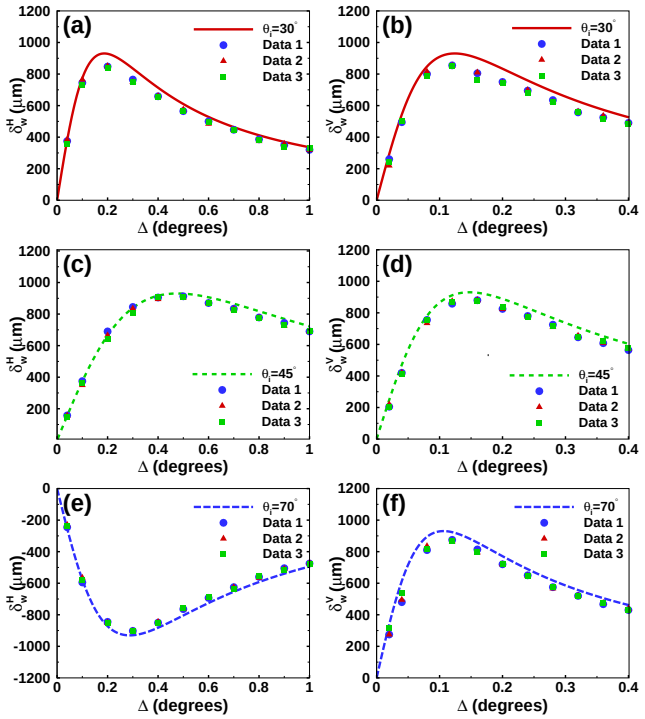

FIG. 2. (Color online) The amplified shifts of photonic SHE changing with the overlap of the preselection and postselection states in the case of horizontal (left column) and vertical polarizations (right column). Here the incident angles are chosen as θ_i=30°, 45°, and 70°. The lines represent the theoretical results. The circles, squares, and triangles show the experimental data.

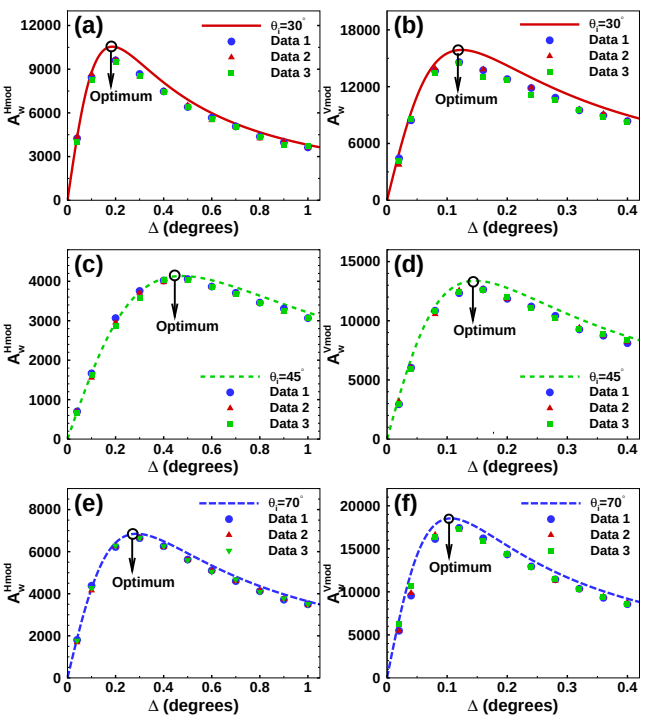

FIG. 3. (Color online) The theoretical and experimental results for selecting the maximum weak value in weak measurements under the condition of preselection and postselection states being almost orthogonal. Here the incident angles are selected as θ_i=30°, 45°, and 70°. The incident states are horizontal (left column) and vertical polarizations (right column). The circles, squares, and triangles denote the experimental data corresponding to the theoretical lines.

modified weak value

$$A_w^{Hmod} = \frac{z_r k_0 r_p^2 \sin(2\Delta)}{(r_p + r_s)^2 \cot^2\Delta \cot^2\theta_i + 2k_0 z_R r_p^2 \sin^2\Delta} \quad (6)$$

$$A_w^{Vmod} = \frac{z_r k_0 r_s^2 \sin(2\Delta)}{(r_p + r_s)^2 \cot^2\Delta \cot^2\theta_i + 2k_0 z_R r_s^2 \sin^2\Delta} \quad (7)$$

Figure 2 shows the amplified displacements of photonic SHE changing with the incident angle θ_i and the degree of overlap of preselection and postselection states (described by the postselection angle Δ). Here, the incident angles are chosen as three fixed values θ_i=30°, 45°, and 70°. We repeat the experiment for three times. The shifts are measured in the case of both $|H\rangle$ and $|V\rangle$ polarizations. Combining with the amplified shifts, we can obtain the amplified factor (modified weak value) in the process of weak measurements as shown in Fig. 3. We surprisingly find that the weak value and amplified displacements can not increase arbitrarily under the orthogonal condition of preselection and postselection states and, on the contrary, it turns out to be zero. Instead, there exists the maximum weak value and amplified displacements with a corresponding optimal overlap of preselection and postselection states. With the maximum weak value, we can get the high measurement precision for probing the photonic SHE. We note that the similar behavior of weak value is investigated in solid-state qubits in which the conditioned average of a finite strength measurement cross through zero at the orthogonality point, and achieve both maximum and minimum values away from this point[29]. In fact, to have the divergence of the weak value, the ordering of the small parameters in weak measurement process must be obeyed. If the ordering of the small parameters is reversed, entirely new physical behavior is expected, and in fact the inverse weak value can appear[30,31].

From Eqs. (6) and (7), using $\frac{\partial A_w^{mod}}{\partial \Delta}$=0, we can get the relationship between incident angle θ_i and postselection angle Δ for obtaining the maximum amplified factor. The results can be seen from Fig. 4 and the preselection states are chosen as $|H\rangle$ and $|V\rangle$ polarizations. We should note that the incident angles can relate to the degree of weak interaction in weak measurements. So, for a fixed incident angle, there exists a maximum amplified factor corresponding to a optimal overlap of preselection and postselection states. In the case of $|H\rangle$ state, a sharp peak [see inset of Fig. 4(a)] appears when the incident angle is close to Brewster angle. Here, we have considered the tiny in-plane spread of wave-vectors in calcula-

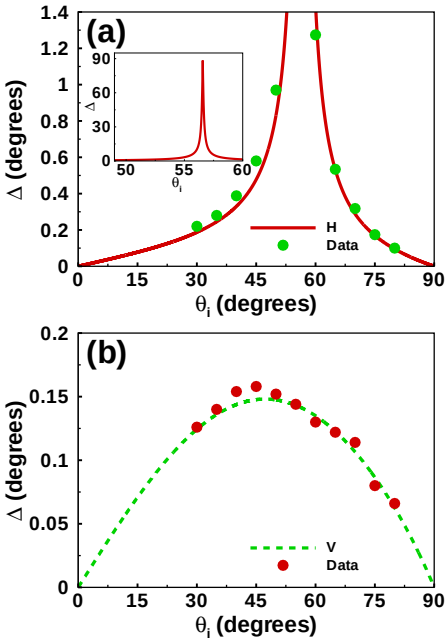

FIG. 4. (Color online) The relationship between incident angle θ_i and postselection angle Δ for obtaining the maximum amplified factor. The incident states are (a) horizontal and (b) vertical polarizations. The circles show the experimental data and the lines denote the theoretical value. The inset describes the sharp value of postselection angle which is not shown in the figure.

tion and not measured postselection angle in this range for the saturation of CCD. In the previous work, the amplified factor presents a valley near the Brewster angle on reflection[9]. From the above analysis, we can select an appropriate amplified factor in weak measurements under the condition of fixed coupling strength, and so the high measurement precision can be obtained. Note that the improvement of the signal-to-noise ratio (SNR) is of great interest in precision metrology. Recently, Jordan *et al*. have done great work to optimize the SNR of a beam-deflection measurement with interferometric weak values[32]. We think that how to optimize the SNR for measuring photonic SHE with the corresponding preselection and postselection states will be an interesting work in the future.

In conclusion, we have used optimal preselection and postselection in weak measurements to detect the photonic spin Hall effect (SHE) for obtaining the high measurement precision. We have proved that there exists the maximum weak value and amplified shift when the overlap of preselection and postselection states are chosen as a corresponding optimal value. We have also considered the orthogonal condition of preselection and postselection states and revealed that the weak value and amplified displacements of photonic SHE can not be arbitrarily large. These findings provide new insight into weak measurements and have possible applications in precision metrology.

We are sincerely grateful to the anonymous referee, whose comments led to significant improvement of our paper. This research was partially supported by the National Natural Science Foundation of China (Grant No. 61025024 and No. 11274106) and Hunan Provincial Innovation Foundation for Postgraduate (Grant No. CX2013B130).

[1] Y. Aharonov, D. Z. Albert, and L. Vaidman, Phys. Rev. Lett. **60**, 1351 (1988).
[2] N. W. M. Ritchie, J. G. Story, and R. G. Hulet, Phys. Rev. Lett. **66**, 1107 (1991).
[3] G. J. Pryde, J. L. O'Brien, A. G. White, T. C. Ralph, and H. M. Wiseman, Phys. Rev. Lett. **94**, 220405 (2005).
[4] J. Dressel and A. N. Jordan, Phys. Rev. Lett. **109**, 230402 (2012).
[5] P. B. Dixon, D. J. Starling, A. N. Jordan, and J. C. Howell, Phys. Rev. Lett. **102**, 173601 (2009).
[6] O. Hosten and P. Kwiat, Science **319**, 787 (2008).
[7] Y. Qin, Y. Li, H. He, and Q. Gong, Opt. Lett. **34**, 2551 (2009).
[8] Y. Gorodetski, K. Y. Bliokh, B. Stein, C. Genet, N. Shitrit, V. Kleiner, E. Hasman, and T. W. Ebbesen, Phys. Rev. Lett. **109**, 013901 (2012).
[9] H. Luo, X. Zhou, W. Shu, S. Wen, and D. Fan, Phys. Rev. A **84**, 043806 (2011).
[10] S. Kocsis, B. Braverman, S. Ravets, M. J. Stevens, R. P. Mirin, L. K. Shalm, and A. M. Steinberg, Science **332**, 1170 (2011).
[11] J. S. Lundeen, B. Sutherland, A. Patel, C. Stewart, and C. Bamber, Nature (London) **474**, 188 (2011).
[12] G. Strübi and C. Bruder, Phys. Rev. Lett. **110**, 083605 (2013).
[13] M. Onoda, S. Murakami, and N. Nagaosa, Phys. Rev. Lett. **93**, 083901 (2004).
[14] K. Y. Bliokh and Y. P. Bliokh, Phys. Rev. Lett. **96**, 073903 (2006).
[15] A. Aiello and J. P. Woerdman, Opt. Lett. **33**, 1437 (2008).
[16] D. Haefner, S. Sukhov, and A. Dogariu, Phys. Rev. Lett. **102**, 123903 (2009).
[17] H. Luo, S. Wen, W. Shu, Z. Tang, Y. Zou, and D. Fan, Phys. Rev. A **80**, 043810 (2009).
[18] N. Hermosa, A. M. Nugrowati, A. Aiello and J. P. Woerdman, Opt. Lett. **36**, 3200 (2011).
[19] N. Shitrit, I. Bretner, Y. Gorodetski, V. Kleiner, and E. Hasman, Nano Lett. **11**, 2038 (2011).
[20] X. Yin, Z. Ye, J. Rho, Y. Wang, and X. Zhang, Science **339**, 1405 (2013).
[21] J.-M. Ménard, A. E. Mattacchione, M. Betz, and H. M. van Driel, Opt. Lett. **34**, 2312 (2009).
[22] X. Zhou, Z. Xiao, H. Luo, and S. Wen, Phys. Rev. A **85**, 043809 (2012).
[23] X. Zhou, X. Ling, H. Luo, and S. Wen, Appl. Phys. Lett. **101**, 251602 (2012).
[24] X. Zhou, J. Zhang, X. Ling, S. Chen, H. Luo, and S. Wen, Phys. Rev. A **88**, 053840 (2013).
[25] R. Jozsa, Phys. Rev. A **76**, 044103 (2007).
[26] T. Geszti, Phys. Rev. A **81**, 044102 (2010).
[27] S. Wu and Y. Li, Phys. Rev. A **83**, 052106 (2011).
[28] X. Zhu, Y. Zhang, S. Pang, C. Qiao, Q. Liu, and S. Wu, Phys. Rev. A **84**, 052111 (2011).
[29] N. S. Williams and A. N. Jordan, Phys. Rev. Lett. **100**, 026804 (2008).
[30] D. J. Starling, P. B. Dixon, N. S. Williams, A. N. Jordan, and J. C. Howell, Phys. Rev. A **82**, 011802 (2010).
[31] D. J. Starling, P. B. Dixon, A. N. Jordan, and J. C. Howell, Phys. Rev. A **82**, 063822 (2010).
[32] D. J. Starling, P. B. Dixon, A. N. Jordan, and J. C. Howell, Phys. Rev. A **80**, 041803 (2009).